Giant Deformations of a Liquid-Liquid Interface Induced by the Optical Radiation Pressure

Alexis Casner* and Jean-Pierre Delville†

Centre de Physique Moleculaire Optique et Hertzienne, UMR CNRS/Universit 5798, Universit Bordeaux I, 351 Cours de la Libration, F-33405 Talence cedex, France

(Received 9 April 2001; published 16 July 2001)

Because of the small momentum of photons, very intense fields are generally required to bend a liquid interface with the optical radiation pressure. We explore this issue in a near-critical phase-separated liquid mixture to vary continuously the meniscus softness by tuning the temperature. Low power continuous laser waves become sufficient to induce huge stationary bulges. Using the beam size to build an "optical" Bond number, Bo, we investigate the crossover from low to large Bo. The whole set of data collapses onto a single master curve which illustrates the universality of the phenomenon.

DOI: 10.1103/PhysRevLett.87.054503 PACS numbers: 47.20.Ma, 42.25.Gy, 42.50.Vk, 82.70.Kj

The interaction between a laser wave and a micrometer-sized dielectric particle has attracted considerable interest in recent years. While most advances were devoted to optical levitation and trapping (for a recent review see, for example, [1]), much less attention appears to have been directed to the deformation of soft transparent interfaces (such as liquid-gas menisci [2] or liquid droplets [3]) despite its large field of practical applications [3–6]. High beam intensities are nevertheless needed to deform classical liquid interfaces. The first investigations were therefore prompted with laser pulses [2], but control over the spatial and temporal profiles of the wave was not very accurate, and secondary disturbing couplings such as nonlinear effects, thermal expansion, or thermocapillary flows [7] generally appear. Moreover, when observed, deformations remain usually weak (typically $\sim$2 nm high for a water-air interface when induced by a cw Ar^+ laser with a beam power $P = 300$ mW and a beam radius $\omega_0 = 140$ μm [4]) and indirect methods, such as induced lensing [2,4] or interferometric holography [6], need to be implemented for measurements.

On the other hand, these optical forces represent nowadays an appealing noncontact tool to probe locally the micromechanical properties of soft biological systems because artificial membranes [8] or cells [9] can be highly deformable. Sizable effects of the radiation pressure should then be measured leading to improvements in surface elasticity characterization. Further developments of these new horizons would therefore require an experimental investigation from the low to the large surface tension regime to present a universal description of the mechanisms that govern the shape and the amplitude of the induced deformations. This is the purpose of the present Letter.

Using a cw laser wave to bend the meniscus between two liquid phases in coexistence close to a liquid-liquid critical point, we show that huge stationary interface deformations of several tens of microns can be induced at low beam power. Moreover, the continuous variation of the surface softness by a scanning in temperature allows a universal description of the phenomenon because it becomes possible to overlap the range of variation of the excitation and the hydrodynamic length scale, respectively, given by the beam waist ω_0 and the capillary length l_C. New predicted behaviors are then seen to occur, particularly the transition from a nonlocal to a local excitation of the interface when the critical point is neared, and all the data can be cast on a single master curve when rescaled with an optical Bond number.

The experiment is performed in a near-critical water-in-oil micellar phase of microemulsion. Its mass composition (water: 9%; sodium dodecyl sulfate: 4%; toluene: 70%; and n-butanol: 17%) has been chosen so as to be critical at a temperature $T_C = 35C$ [10]. For a temperature $T > T_C$ the mixture phase separates in two micellar phases of different micellar concentrations. Four main reasons motivated our choice. (i) Close to the liquid-liquid critical point, this micellar phase belongs to the universality class ($d = 3, n = 1$) of the Ising model [10]; very general conclusions can thus be devised by our investigation. (ii) The amplitude of the correlation length of density fluctuations is intrinsically large in supramolecular liquids: in the one-phase region of our mixture $\xi^+ = \xi_0^+|1 - \frac{T}{T_C}|^{-\nu}$, with $\xi_0^+ = 40 \pm 2$ Å and $\nu = 0.63$. Consequently the critical amplitude σ_0 of the surface tension is very weak compared to that of usual liquid mixtures ($\sigma = \sigma_0|1 - \frac{T}{T_C}|^{2\nu}$ with $\sigma_0 = \frac{k_B T_C R^+}{(\xi_0^+)^2}$ and $R^+ = 0.39$ [11]). (iii) The refractive index contrast between the coexisting micellar phases is important in the chosen microemulsion. (iv) Finally, the very weak residual absorption of the mixture at the wavelength used and the low incident beam powers needed to observe the interface bending prevent any disturbing thermal coupling and nonlinear effect [10].

A schematic of the experiment is presented in Fig. 1. The mixture is enclosed in a temperature controlled parallelepipedic fused quartz cell (optical path of 1 mm, 1 cm wide), and the working temperature T is chosen above T_C to reach a two-phase equilibrium state. Since the density of water is larger than that of toluene, the high micellar concentration phase Φ_1 is located below the low micellar concentration phase Φ_2 in the gravity field $\vec{g}$. The deformation of the flat meniscus is driven by a linearly

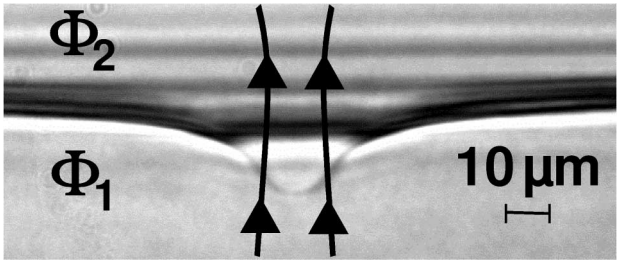

FIG. 1. Optical bending of the meniscus of a phase-separated liquid mixture induced by the radiation pressure. The laser beam is represented by the arrows.

polarized cw Ar^+ laser in the TEM_{00} mode (wavelength in vacuum $\lambda_0 = 5145$ Å propagating vertically from Φ_1 to Φ_2 along the z axis. The wave is weakly focused on the interface by a 10× microscope objective. Thus the beam profile has almost a cylindrical symmetry around the z axis and close to the meniscus the z variation of the beam intensity $I(r,z)$ can be neglected, leading to $I(r,z) \approx I(r) = \frac{2P}{\pi\omega_0^2}\exp(\frac{-2r^2}{\omega_0^2})$ where P is the incident beam power. The beam waist ω_0 can also be changed by adjusting the distance between a first lens ($f = 200$ mm) and the 10× objective. Relative errors on P and ω_0 are, respectively, $\frac{\triangle P}{P} \leq 5\%$ and $\frac{\triangle\omega_0}{\omega_0} \leq 5\%$.

Since the refractive index n_2 of the phase Φ_2 is larger than n_1 of Φ_1 (the refractive index of water is smaller than that of toluene), the light momentum in Φ_2 is larger than that in Φ_1. This light momentum discontinuity at the interface gives birth to a radiation pressure directed towards the coexisting phase of lower refractive index, i.e., Φ_1 in our case. As a result, the radiation pressure acts downwards (see Fig. 1) and should be compensated by the Laplace and the buoyancy forces. Then, at steady state and for a small curvature of the bending, the height of the resulting stationary deformation $h(r)$ is described by [12]

$$(\rho_1 - \rho_2)gh(r) - \sigma\vec{\nabla}^2 h(r) = \frac{2n_1}{c}\left(\frac{n_1 - n_2}{n_1 + n_2}\right)I(r), \tag{1}$$

where ρ_1 and ρ_2 are the densities of the phases Φ_1 and Φ_2, and c is the light velocity in vacuum. The right-hand side term in Eq. (1) represents the radiation pressure $p_{\rm rad}$ at the interface. A typical evolution of $h(r)$ for increasing beam power P is presented in Fig. 2.

Assuming $\vec{\nabla}^2 h(r) \sim \frac{h}{\omega_0^2}$, the ratio between the buoyancy and the Laplace restoring forces defines an optical Bond number $Bo = (\frac{\omega_0}{l_C})^2$, where $l_C = \sqrt{\sigma/(\rho_1 - \rho_2)g}$ is the capillary length. This definition simply means that the induced bulge can be viewed as a sort of virtual particle of length scale ω_0. For optical bending of classical free surfaces $Bo \ll 1$ and gravity is negligible. Then one finds

$$h(r=0)_{Bo\ll 1} = \left(\frac{\partial n}{\partial\rho}\right)_T \frac{1}{4\pi g}\ln\left(\gamma\,\frac{\omega_{cl}^2}{\omega_0^2}\right)\frac{P}{l_C^2}, \tag{2}$$

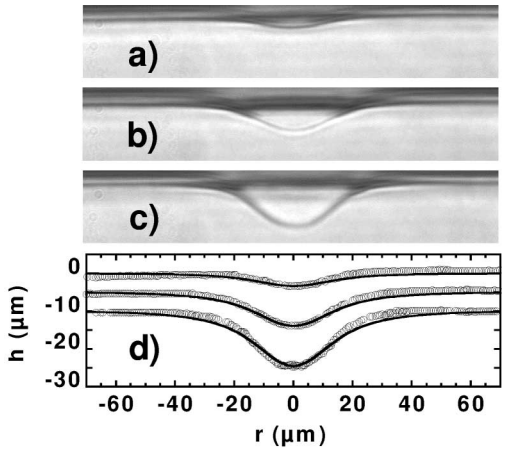

FIG. 2. Variation of the optical bending for increasing beam power: (a) $P = 270$ mW, (b) 540 mW, (c) 810 mW. (d) Theoretical profiles (full lines) calculated from Eq. (4). The control parameters are $\omega_0 = 14.6$ μm and $(T - T_C) = 2$ K.

where $\gamma = 1.781$ is the Euler constant and ω_{cl} is a radius large compared to ω_0 that defines the boundary condition $h(r = \omega_{cl})_{Bo\ll 1} = 0$. We have also assumed here that $n_1 \simeq n_2$ and $(n_1 - n_2) = (\frac{\partial n}{\partial\rho})_T(\rho_1 - \rho_2)$ because Φ_1 and Φ_2 are coexisting phases of close compositions. Equation (2) shows that the deformation strongly depends on l_C rather than ω_0: the response of the interface to the radiation pressure is thus nonlocal [i.e., $\vec{\nabla}^2 h(r) \propto I(r)$]. Data should therefore be plotted versus $\frac{P}{l_C^2}$ to point out a single-scaled behavior, rather than $p_{\rm rad}(r=0) \propto \frac{P}{\omega_0^2}$ used generally [2]. In our case, this behavior can be observed experimentally using a narrow beam excitation in the two-phase sample far from criticality. The expected scaling is illustrated in Fig. 3 for large values of $(T - T_C)$. For a comparison the inset shows the dispersion of the same data when plotted versus $\frac{P}{\omega_0^2}$. Since the relative error on ξ_0^+ is $\frac{\triangle\xi_0^+}{\xi_0^+} = 5\%$ and $(T - T_C)$ is regulated at better than 0.1 K, we deduce $\frac{\triangle l_C^2}{l_C^2} \leq 11\%$ for $(T - T_C) \geq 8$ K; measurements give $\frac{\triangle h}{h} \leq 10\%$.

On the other hand, when $Bo \gg 1$ the Laplace force becomes negligible and the height of the deformation is simply given by

$$h(r=0)_{Bo\gg 1} = \left(\frac{\partial n}{\partial\rho}\right)_T \frac{1}{cg}\,I(r=0)\,. \tag{3}$$

The optical excitation of the interface induced by the radiation pressure becomes local [i.e., $h(r) \propto I(r)$]. Data should therefore be plotted in $\frac{P}{\omega_0^2}$ to obtain a scaled description of the height of the bulge. This behavior, which seems to have never been analyzed before, is, in fact, difficult to observe. The main reason is that experiments should be realized with large beam radii, but in such conditions the beam intensity decreases drastically and the deformation becomes too weak to be accurately detected. Besides

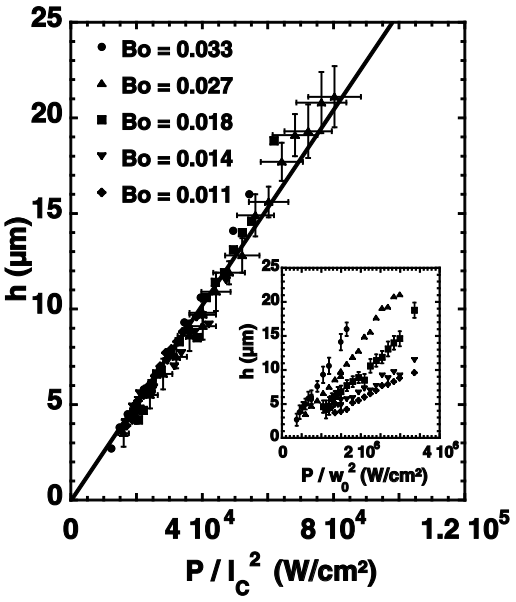

FIG. 3. Experimental variation of the height of the deformation for low optical Bond numbers. The single-scaled behavior predicted by Eq. (2) is clearly evidenced. Inset: same data when plotted versus $\frac{P}{\omega_0^2}$. The control parameters are $\omega_0 = 6.3\ \mu$m and $(T - T_C) = 8$ K (•), 10 K (▲), 15 K (■), 20 K (▼), and 25 K (◆).

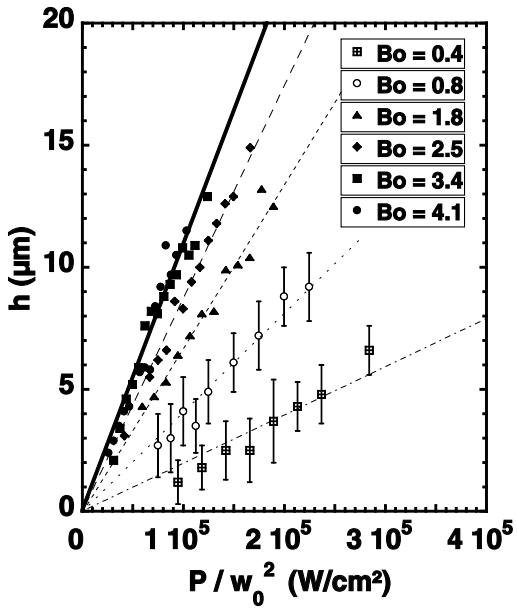

FIG. 4. Experimental variation of the height of the deformation for optical Bond numbers increasing from the intermediate to the large Bo regime. The predicted scaling given by Eq. (3) for $Bo \gg 1$ is illustrated by the full line. The control parameters are $(T - T_C) = 1.5$ K and $\omega_0 = 10.6\ \mu$m (⊞), 14.6 μm (○), 21.2 μm (▲), 25.3 μm (◆), 29.3 μm (■), and 32.1μm (•).

a strong increase in beam power generally initiates disturbing nonlocal couplings like thermal effects [7]. With near-critical phase-separated liquid mixtures, the situation is more comfortable because the capillary length vanishes when approaching the critical point. Then, the transition towards the negligible surface tension limit can be investigated. Using large beam waists at $(T - T_C) = 1.5$ K, Fig. 4 shows that the slope of $h(r = 0)$ versus $\frac{P}{\omega_0^2}$ increases for increasing Bo and reaches progressively a finite value for $Bo > 1$. This behavior is clearly evidenced by the two largest Bo presented.

To analyze more quantitatively the universal behavior of optical bending of soft interfaces we solved Eq. (1). Introducing the Fourier-Bessel transform $h(r) = \int_0^\infty \tilde{h}(k) J_0(kr) k\, dk$ [2], where $J_0(x)$ is the 0th order Bessel function, one finds

$$h(r) = \left(\frac{\partial n}{\partial \rho}\right)_T \frac{P}{2\pi c g} \int_0^\infty J_0(kr) \frac{\exp(-\frac{k^2\omega_0^2}{8})}{1 + k^2 l_C^2}\, k\, dk\,. \quad (4)$$

The nice feature from Eq. (4) is that $h(r = 0)$ can be derived analytically [13] in a universal form of the Bond number:

$$h(r = 0) = [h(r = 0)]_{Bo \gg 1} \times F(Bo), \quad (5)$$

where $F(x) = \frac{x}{8} \exp(\frac{x}{8}) E_1(\frac{x}{8})$, $E_1(x)$ is the exponential integral function, and $[h(r = 0)]_{Bo \gg 1}$ is given by Eq. (3). The remarkably simple form of Eq. (5) provides a natural scaling for presenting the data. The whole set of experiments should be brought onto a single master curve when expressed with the reduced variables Bo and $H = \frac{h(r=0)}{[h(r=0)]_{Bo \gg 1}}$. Figure 5 presents this data rescaling for a very wide region of the parameter space: $0.06 \leq P \leq 1.2$ W, $5.3 \leq \omega_0 \leq 32.1\ \mu$m, $1.5 \leq (T - T_C) \leq 25$ K, corresponding to almost three decades in optical Bond number in a range including $Bo = 1$. Using the estimation of $\frac{\triangle l_C^2}{l_C^2}$ given above, the error on Bo is $\frac{\triangle Bo}{Bo} \leq 15\%$ for $(T - T_C) \geq 1.5$ K; measurements lead to $\frac{\triangle H}{H} \leq 8\%$. All the data are closely distributed around the solid line which represents the scaling function $F(Bo)$. For given ω_0 and $(T - T_C)$, each point is deduced from the slope value of the linear variation of $h(r = 0)$ versus $I(r = 0)$. The only free parameter $(\frac{\partial n}{\partial \rho})_T$ is obtained by fitting in the least squares sense the full set of experimental points. We find $(\frac{\partial n}{\partial \rho})_T = -1.22 \times 10^{-4}\ \mathrm{m^3\,kg^{-1}}$, a value somewhat larger than that expected from the Clausius-Mossotti relation $[(\frac{\partial n}{\partial \rho})_T = -6.1 \times 10^{-4}\ \mathrm{m^3\,kg^{-1}}]$. For the sake of comparison, the datum given by Sakai *et al.* [4] for the water-air free surface at room temperature ($H = 1.9 \times 10^{-3}, Bo = 2.7 \times 10^{-3}$) is also illustrated in the inset of Fig. 5. It shows that the universal scaling function $F(Bo)$ makes predictable the height of the laser-induced deformation, whatever the liquid interface is.

Finally Eq. (4) was used to compare predictions with the entire profile of the stationary deformation $h(r)$ measured experimentally. Considering the value of $(\frac{\partial n}{\partial \rho})_T$ obtained above, Fig. 2 shows that the expected bendings fairly reproduce observations. The measurement of $h(r = 0)$ is thus sufficient to completely describe the shape distortion induced by the radiation pressure.

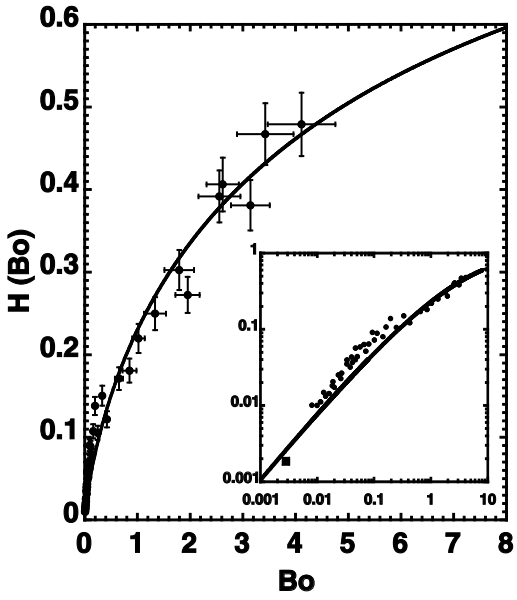

FIG. 5. Experimental variation of the dimensionless height of the deformation $H(Bo)$ versus the optical Bond number. The solid line represents the universal scaling function $F(Bo)$ given in Eq. (5). Inset: log-log plot overview, which also shows the location of the datum (full square) given in Ref. [4] for the water-air free surface.

In conclusion, the good agreement observed between the scaled function $F(Bo)$ and our measurements — and others on free surfaces — clearly validates the universal description of the process, and provides a new example of the convenience offered by critical phenomena to explore hydrodynamic instabilities and pattern formation [14].

We are grateful to P. Panizza for helpful discussions, and to J. Plantard and M. Winckert for technical assistance. We thank B. Mallet for preliminary studies. This work was partly supported by the Conseil Regional d'Aquitaine.

*Electronic address: acasner@cribx1.u-bordeaux.fr
†Electronic address: delville@cribx1.u-bordeaux.fr

[1] A. Ashkin, Proc. Natl. Acad. Sci. U.S.A. **94**, 4853 (1997).
[2] A. Ashkin and J. M. Dziedzic, Phys. Rev. Lett. **30**, 139 (1973); H. M. Lai and K. Young, Phys. Rev. A **14**, 2329 (1976).
[3] J. Z. Zhang and R. K. Chang, Opt. Lett. **13**, 916 (1988); H. M. Lai *et al.,* J. Opt. Soc. Am. B **6**, 2430 (1989); I. Brevik and R. Kluge, J. Opt. Soc. Am. B **16**, 976 (1999).
[4] K. Sakai *et al.,* Phys. Rev. E **63**, 046302 (2001).
[5] A. V. Katz and V. M. Kontorovitch, Sov. Phys. JETP **41**, 346 (1975).
[6] I. I. Komissarova *et al.,* Opt. Commun. **66**, 15 (1988).
[7] S. A. Viznyuk and A. T. Sukhodol'skii, Sov. J. Quantum Electron. **18**, 489 (1988); A. A. Kolomenskii and H. A. Schuessler, Appl. Opt. **38**, 6357 (1999).
[8] R. Bar-Ziv *et al.,* Biophys. J. **75**, 294 (1998).
[9] J. Guck *et al.,* Phys. Rev. Lett. **84**, 5451 (2000).
[10] E. Freysz *et al.,* Phys. Rev. E **49**, 2141 (1994).
[11] M. R. Moldover, Phys. Rev. A **31**, 1022 (1985).
[12] I. Brevik, Phys. Rep. **52**, 133 (1979).
[13] M. Abramowitz and I. A. Stegun, *Handbook of Mathematical Functions* (Dover Publications Inc., New York, 1972).
[14] J. V. Maher, Phys. Rev. Lett. **54**, 1498 (1985); S. Fauve *et al.,* Phys. Rev. Lett. **68**, 3160 (1992); M. Assenheimer and V. Steinberg, Phys. Rev. Lett. **70**, 3888 (1993); A. B. Kogan *et al.,* Phys. Rev. Lett. **82**, 4635 (1999).